Proceedings World Geothermal Congress 2010
Bali, Indonesia, 25-29 April 2010

Laboratory Results of Corrosion Tests for EGS Soultz Geothermal Wells

Jiri Muller[1], Katerina Bilkova[2], Albert Genter[3] , Marion Seiersten[4]

IFE, Norway; IFE, Norway; GEIE EMC, France; IFE Norway

[1]jiri.muller@ife.no; [2]katerina.bilkova@intecha.cz; [3]genter@soultz.net; [4]marion.seiersten@ife.no

Keywords: Corrosion risk, corrosion test, corrosion protection, inhibitor, protective coating, EGS, Soultz-sous-Forêts

ABSTRACT

Corrosion risk for the materials (casing, pipes) proposed for the Soultz project at 200°C was evaluated in laboratory in order to estimate the corrosion rate before the beginning of the geothermal power plant running. After a short review about the both corrosion and scaling works done at Soultz, detail laboratory experiments are fully described and interpreted in high temperature conditions. The tested materials were: steels TU42BT, P110, N80, steel with Sakaphen coating, and steel with two types of Teflon coating. The corrosion tests showed that carbon steel TU42BT corroded at 2 mm/y at 200°C. The corrosion products formed on the surface did not provide any corrosion protection. All the tested coatings performed very well. They effectively reduced the corrosion and they did not deteriorate during the test. Mexel inhibitor, which was tested in the past on-site but at lower temperature (<150°C) did not give any significant inhibitor effect at 200°C. The corrosion rate for TU42BT steel was nearly the same with and without the inhibitor indicating that new generation inhibitor must be recommended. The outside top part of the casing was investigated for microbiological corrosion.

1. INTRODUCTION

The Soultz EGS (Enhanced Geothermal Systems) project which is located in Eastern part of France has been running for more than 20 years involving French, German, Norwegian and Swiss scientists. Main geoscientifc achievements take into account the deep-seated geology of a hidden crystalline basement penetrated by several deep geothermal wells (Genter et al., 2010; Gérard et al., 2006). Three deep wells have been drilled to 5 km into a granite reservoir, cased between the surface and 4.5 km depth which were stimulated hydraulically and chemically (Hettkamp et al., 2004, Nami et al., 2008). Then, several hydraulic circulation tests have been conducted with the geothermal triplet in order to test the hydraulic performance of a deep fractured reservoir (Gérard et al., 2006). GPK2 and GPK4 wells, which are equipped with down-hole submersible pumps, are used for production and GPK3 well is used for re-injection (Fritsch et al., 2008). Then, an Organic Rankine Cycle (ORC) power plant has been built recently and is still in its learning curve with a net power capacity of 1.5 MWel (Fritsch et al., 2008; Genter et al., 2009).

Drilling operations have shown the presence of native brine percolating within the natural fracture network (Aquilina et al., 1997; Vuataz et al., 1990). The most relevant geochemical data on the nature of these fluids show that fluid samples collected in different Soultz wells have similar chemical and isotopic compositions characterized by NaCl brine containing CO2 with a pH value close to 5 at high temperature conditions (Sanjuan et al., 2010). The high salinity of the Soultz brine (100 g/l), which is very corrosive, has to be taken into account for the life-time of the surface geothermal installations and the cased parts of the wells.

Corrosion and scaling studies in actual geothermal conditions have not been investigated intensively on site during the early Soultz phases (Baticci et Faucher, 2008; Baticci, 2009; Baticci et al., 2010). In 1994, studies about corrosion of the drill pipes were conducted with the first encouraging work by testing successfully the Mexel 432 inhibitor with a carbon steel ring immerged within the geothermal brine for reducing metal loss. This inhibitor is a multi-functional water treatment product based on filming amine technology.

In 1997, during a 4-month circulation test in the 3.6 km depth reservoir, this inhibitor was again used for protecting the different geothermal equipments (casing, down-hole pump) and monitored the behaviour of some steels. The inhibitor was injected a rate of 4 kg per day at the pump intake within the production well at high temperature (142°C). At re-injection temperature conditions (65°C), an on-site corrosion tool was installed for monitoring the behaviour of 4 different materials (Hastelloy, Uranus B6, 316L stainless steel, K55). No evidence of corrosion was observed on the production pump (Baticci and Faucher, 2008). On surface, a very low corrosion rate was observed on the carbon steel (K55) coupon only. Some scaling (galena, magnetite) were also observed in the surface filtering system by x-ray diffraction analysis.

In 2005, during a 5-month circulation test in the 5 km depth reservoir, resistance to corrosion was tested by immerging different steel samples (P110, N80) in the produced geothermal brine. A mass loss of about half mm per year was outlined. However, this value was may be underestimated because of a general grease filming protection of the samples due to well-head pack-off systems. In the well, some borehole image logs have been run in the cased part of the triplet (Baticci et Faucher, 2008). Corrosion was only suspected in some limited depth sections were borehole ovalisation could occurred. On surface, galena and magnetite were again observed as a scaling deposit.

In 2008, some scaling deposits, mainly galena and sulfate were also observed on the production down-hole used in GPK2 which has been pulled off, on surface in re-injection conditions in the filtering system or in the corrosion pilot system (Baticci, 2009).

Thus, it was decided to test experimentally at high temperature conditions (200°C), the reaction of different steels from the heat exchanger (TU42BT) and from the casing (P110, N80) in contact with a Soultz brine composition. In order to propose some solutions and recommendations for reducing the anticipated corrosion rate, different coatings were also tested experimentally at laboratory conditions. Sakaphen coating which is a resin as well as 2 different types of Teflon were tested for the first time at 200°C. Thus, this paper reports the results of the first

corrosion experiments at high temperature conditions with the different steels used at Soultz (casing, pipe, heat exchanger) and coatings that may be used.

The main objective of the tests was to evaluate the corrosion risk for the materials proposed for Soultz project at 200°C and to evaluate the Mexel corrosion inhibitor. The tested materials were: steels TU42BT, P110, N80, steel with Sakaphen coating, and steel with two types of Teflon coating. The evaluation was performed in synthetic brine in an autoclave. An additional evaluation of the Mexel corrosion inhibitor was done in a glass cell tests at ambient pressure at 60ºC.

2. CORROSION TESTS

2.1 Experimental Procedure

2.1.1 Autoclave Tests

The corrosion tests were carried out in a Hastelloy C autoclave. The schematic drawing is shown in Figure 1. The autoclave was equipped to house specimens of various geometries and to allow electrochemical measurements. Two tests were carried out, one without and one with Mexel inhibitor. The test matrix is given in Table 1. Three types of steel were tested: carbon steel TU42BT, low carbon steels P110, and N80. Steels P110, and N80 were tested only in the second test, EGS_03. The non-coated steel specimens were ground with series of SiC papers up to 1000 mesh wetted with isopropanol, cleaned in an ultrasonic bath with technical acetone and flushed with ethanol. The specimens were blow dried, weighed and mounted on the specimen holders. The chemical composition of the steels is given in Table 2. Detailed chemical composition for the P110 and N80 steels was not available. In the first test, EGS_02, three organic coatings were tested along with TU42BT steel, the coatings were: Sakaphen synthetic coating, and two types of Teflon coating. The Teflon coatings were named after the colour of the coating: Teflon green, and Teflon red. These coatings have never been tested at high temperatures with saline fluid. All experiments were carried out in artificial brine with the same ionic composition as the produced brine from the well. The chemical composition of the brine is given in Table 3. The solution was purged continuously with carbon dioxide to avoid oxygen ingress prior to the test. The carbon dioxide partial pressure was 0.5 bar. The tests were carried out at 200°C, where the total pressure was 15 bar. The concentration of Mexel inhibitor was 10 ppm. The pH was 4.6 at the start, and it increased to 5 during the test. The pH was measured at room temperature. The iron content at the end of the tests was 15 ppm in the first test, EGS_02, and 60 ppm in the second test, EGS_03.

Gamry PCI4 potentiostat with a multiplexer was used for electrochemical measurements. The specimen and the other electrodes were connected to the potensiostat with insulated wires. The connections were done by drilling a 1 mm deep hole with the same diameter as wire in the electrodes, connect the wire in the hole and fix it by indentation. The connection point was painted to avoid exposing the wire to the solution. The corrosion rate was monitored by linear polarization resistance (LPR) throughout the test. LPR measurements were performed in three-electrode configuration, i.e. working electrode - carbon steel specimen, reference electrode - carbon steel, auxiliary electrode - Ti ring. The potential ramp for the LPR measurement was –5 mV to +5 mV vs. the open circuit potential with scan rate 0.1 mV/s. The corrosion currents was calculated as B/Rp, with B = 20 mV, and converted to average corrosion rates according to standard procedure for LPR measurements (1A/m2 corresponds to 1.16 mm/y) during the test. After the test, the corrosion rate measured by LPR was calibrated by the mass loss measurements and compensated for IR drop. This gave individual B values for each test. The solution resistance for IR drop compensation was determined by means of impedance spectroscopy (EIS) towards the end of the test. The EIS was carried out in the frequency range 5000 Hz to 100 mHz, with amplitude 5 mV rms. The IR drop was measured towards the end of the experiment to avoid disturbing the corroding specimen

during the test. It might change during the test, but the change does not affect the overall measured corrosion rate. The IR drop is negligible compared to the overall corrosion resistance for well inhibited specimens. It can be a considerable part of the corrosion resistance for non inhibited specimens, but then there is no corrosion film that contributes to the IR drop.

Mass loss corrosion rates were determined according to ASTM Standard Practice G 1-90 (Fazio, 1992). **T**hey were calculated from the weight difference, Δm, of the steel before exposure, m1, and after exposure and removal of corrosion products, m2.

$$\Delta m = m1-m2 \quad (1)$$

The corrosion rate was calculated

$$C.R. = k\Delta m/(AtD) \quad (2)$$

where k is a constant, A is the area of the electrode, t is the time of exposure, and D is density of the metal.

The weight of the corrosion product film, Δmfilm was calculated as difference between the weight after the exposure, m3, and the weight after corrosion product removal, m2

$$\Delta mfilm = m3-m2 \quad (3)$$

Corrosion products were removed in inhibited HCl. The inhibited HCl is concentrated HCl, which contains 50 g/l $SnCl_2$ and 30 g/l $SbCl_3$. This solution is routinely used for removing corrosion products chemically without affecting the metal.

At the end of the exposure the specimens were inspected by optical microscopy for the nature of the corrosion attack and any occurrence of localized attack. The composition of the corrosion product films and precipitates was examined by Scanning Electron Microscopy (SEM), and by Energy Dispersible X-ray Spectroscopy (EDS).

No polarisation resistance measurements could be performed on the coated specimens because the coatings were non-conductive. The corrosion of these specimens was evaluated by mass loss and by the inspection of the specimens by means of optical microscopy and SEM as described above.

2.1.2 Glass Cell Test

One glass cell test was carried out to determine the effect of the Mexel corrosion inhibitor at moderate temperature (60 C). The reason was that the inhibitor did not give any effect in test EGS_03 at 200 C. The glass cell test was carried out in glass cells with a volume of 3 litres. Electrodes for electrochemical corrosion monitoring and pH measurements, temperature probes and gas inlets/outlets were inserted through stainless steel lids. The glass cell with accessories is schematically represented in Figure 2. A

heating plate heated the cell. Magnetic stirring provided convection. The test was carried out at 60°C, with CO_2 partial pressure of 0.8 bar (1.01 bar total pressure and 0.2 water vapour pressure). The test solution was the same as for the previous tests; the composition is given in Table 3. The inhibitor concentration was 10 ppm. Two specimens were immersed in the cell. The specimens were cleaned and prepared before the test in the same way as the specimens for the autoclave tests. The inhibitor was added after 4 hours of precorrosion. The corrosion rate measurement was the same as for the autoclave tests.

3. RESULTS

3.1 Autoclave Tests

3.1.1 Test EGS_02

The mass loss corrosion rates for all the specimens are given in Table 4. Mass of the corrosion product film for the non-coated steel is also given in Table 4. The corrosion rate for the non-coated carbon steel was quite high, 1.8 mm/y. Mass loss corrosion rate for the specimen with Sakaphen coating was marginal; 0.034 mm/y. There were no visible defects in the coating that could explain the weight loss, and it may be speculated that the weight loss is a slight dissolution or loss of solvent. There was not detectable mass loss for the two Teflon coatings. All coatings seemed to provide very good protection against corrosion at the tested conditions.

The development of the corrosion rate measured by LPR for the non-coated steel specimen in the course of the test is given in Figure 3. The corrosion rate stabilized at about 1.9 mm/y after 70 hours of exposure and was stable for the rest of the test. Inspection of the specimen after the test showed that the specimen was covered with black corrosion products (Fig. 4). The corrosion product layer consisted of fine crystals of iron oxide and it was quite porous and from 6 to 35 μm thick (Fig. 5). EDS analysis gave iron/oxygen ratio about 0.4 in the film (Fig. 6). (The carbon content (4 wt%) is apparent; it is due to the carbon film applied on the samples to make them conductive for the SEM and EDS analyses).The ratio was lower than for either magnetite or ferrous oxide. The corrosion product layer was thus probably a hydrated iron oxide. The corrosion product layer was not protective, because the corrosion was not effectively reduced by the deposition of the layer.

The photographs of the specimens with coatings are given in Figures 7-9. SEM images of the cross sections of the specimens with coatings are given in Figures 10-12. None of the coatings seemed to deteriorate during the test. No blisters or detachment of the coatings were observed. The inclusions in the metal near the interface to the Sakaphen coating come from the manufacturing of the coating (Fig. 10), they are not corrosion products; EDS analysis showed that they contain silica. The origin of the silica is most probably that the specimens are sand blasted prior to coating.

3.1.2 Test EGS_03

The mass loss corrosion rates and the mass of the corrosion product films for all the specimens are given in Table 4. The mass loss rate for TU42BT steel was 1.4 mm/y, which was nearly the same as for the test without inhibitor. Thus the inhibitor did not reduce the corrosion significantly. The corrosion rates for the other steels, P110, and N80 was also high, 2.5 mm/y.

The development of the corrosion rate measured by LPR for the non-coated steel specimens in the course of the test is given in Figure 13. Unfortunately a contact with the reference electrode was lost after 50 hours, so no more LPR data were obtained after that. But the experiment was continued for one more week. The corrosion rate after 50 hours was about 4 mm/y for all the specimens. This is, however, not corrected by weight loss measurements and as these give a lower average rate, the corrosion rates must either have been much lower towards the end of the experiment or lower throughout the test.

Inspection of the specimens after the test showed that all the specimens were covered with black corrosion products (Figs. 14-16). Inspection of cross sections of the specimens showed that the corrosion products consisted of several layers (Figs. 17b-c, 18b-c, 19b). The layer on the surface mainly consisted of cubic crystals as is clear from the SEM images of the specimen surface (Figs. 17a, 18a, 19a). EDS analysis is given in Figures 20-22. The iron/oxygen ratio was in the range 0.2-0.3, which indicates carbonate and is too low for magnetite and for ferrous oxide. Iron carbonate is, however, not expected to form at 200°C (Gérard et al., 2006) and the corrosion products thus probably consisted of mixed iron carbonate, calcium carbonate and hydrated ferrous oxide. It cannot be excluded that some $FeCO_3$ has precipitated on the surface during cooling after the test (the specimens could not be removed at 200°C; hence the specimens were cooled to room in the test solution before removing).

3.1.3 Glass Cell Test

The development of the corrosion rate measured by LPR is given in Figure 23. 10 ppm Mexel inhibitor was added after 4 hours. Addition of the inhibitor did not have any effect on the corrosion rate. The inhibitor thus did not give any inhibitor effect at 60 C at this concentration.

4. DISCUSSION

The results of the autoclave tests showed that the corrosion rate at these conditions is rather high; in the range 1.5-2.5 mm/y on average. The high corrosion rate and the subsequent SEM investigation demonstrated that no protective film of corrosion products formed at the surface. There were corrosion products at the surface, but these were porous and seemed to consist of ferric or ferrous hydroxides or oxy-hydroxides rather than Fe_3O_4 or $FeCO_3$ that may form protective films. The specimens from the EGS_03 seemed to have more corrosion product on the surface than the specimens form experiment EGS_02.

The Eh-pH diagram (Poubaix diagram) in Figure 24 shows that it is magnetite (Fe_3O_4) rather than siderite ($FeCO_3$) that is stable at 200°C (the metastable hydroxides and oxy-hydroxides are not shown in the figure). Its stability depends on pH and ferrous (Fe^{2+}) concentration in the solution. The pH range in the experiment is indicated by an overlay in the figure. It was measured to 4.5-4 at room temperature. The actual value at 200°C is uncertain. It is probably lower as the dissociation constant of water is only 11.3 at 200°C and the solution will contain carbonic acid as it is in equilibrium with 0.5 bar CO_2. The diagram in Figure 24 thus indicates that an iron concentration of more than 1E-5 m (56 ppm) is needed before Fe_3O_4 starts to form and more will be needed to form a stable film. The iron concentration at the end of the autoclave tests was 15 ppm in EGS_02 and 60 ppm in EGS_03 which implies that Fe_3O_4 might form in EGS_03. The difference in iron concentration at the end of the two tests is due to three corroding samples in EGS_03 and only one in EGS_02.

The reason for the high corrosion rate in the autoclave tests seems thus to be a low pH and a low concentration of dissolved iron. There is not much relevant data in the literature for purely sweet (no H_2S) geothermal wells. The reports that are available indicates that the pH should be well above 4.5 to form magnetite and hence use carbon steel without further corrosion inhibition (Litchi et al., 1997; Litchi et Wilson, 1999; Sampedro et al., 1990; Sanada et al;, 2000).

As there are seemingly no protection from oxide films at these conditions corrosion inhibitor must be applied. One inhibitor was tested at these conditions; Mexel. It did not affect the corrosion rate at the applied concentration (10 ppm) and the effects seen on the corrosion products when comparing experiment EGS_02 and EGS_03 might as well be explained by the change in solution chemistry; both the iron concentration and the alkalinity is higher in EGS_03 due to a larger corroding area (more specimens). The Mexel inhibitor did not lower the corrosion rate in the more benign conditions in the glass cell test either.

The corrosion rates derived from laboratory tests indicate a rather high value of about 2 mm per year at high temperature. The casing thickness being around 8 mm in most of the Soultz wells, this high corrosion rate would have been able to deteriorate the complete casing section over 4 years. This simple extrapolated calculation is quite unrealistic because most of the Soultz casing is older than 6 years (Hettkamp et al., 2004). A complete survey of four deep wells (GPK1, GPK2, GPK3, GPK4) cumulating more than 16 km length of steel pipes, has been done by using borehole image logs in 2005. No significant issue has been observed at that time in terms of corrosion within those four geothermal wells. However, as the temperature conditions are below 200°C in most casing sections most of the time that could partly explain a lower corrosion rate. The stagnant conditions in-non running periods can also be an explanation.

The use of coating seems a promising way for protecting pipes and tubing in geothermal energy. Based on that laboratory study, Sakaphen has been fully deployed within the Soultz tubular heat exchangers which are now installed. Teflon has not been used yet as a protecting coating within the Soultz power plant. Sakaphen could also be a promising coating product and could be recommended for protecting the down-hole production pump currently running at Soultz.

The corrosion inhibitor did not show promise results with the given laboratory conditions. However, this inhibitor was successfully used at Soultz, but below 150°C. A new generation of inhibitor is needed and has to be tested and used at high temperature mainly for protecting the down-hole pump system and the casings.

5. INVESTIGATION OF MICROBIOLOGICAL CORROSION

During pack-off maintenance job on the injection well GPK3 of the Soultz-sous-Forêts project, important traces of corrosion products were found on the outside top part of the casing (Figure 24). It was found that the corrosion took place 2 meters below the casing top end, on the outside part of the pack-off assembly. Because the temperature of the geothermal brine was quite low, 70ºC, it was suspected that the pitting corrosion might be microbiologically induced. Photograph of the corroded part is shown in Figure 25. The corroded specimen was analysed for bacteria by means of two methods: ATP measurement and by cultivation in SRB medium. The first method, ATP measurement, is based on spectrophotometric measurement of a complex of adenosine triphosphate (ATP) with an enzyme. Adenosine triphosphate is present in all living cells and can be used as a measure of bacterial activity. The results of the ATP measurement gave ATP concentration of 10-9 g/l, which indicated very low bacterial activity. The second method was based on cultivation in a medium specific for sulphate reducing bacteria (SRB). When SRB is added to this medium they will reduce sulphate to sulphide, and sulphide will precipitate as black iron sulphide. The medium was incubated for 4 weeks at 30ºC, then iron sulphide is inspected in various dilutions and the number of bacteria are estimated from a standard MPN table. This second analytical method gave concentration of SRB of 4.6 cell/cm^2. The result shows that there were bacteria present on the specimen. Most probably the bacteria came from the corrosion products. This is also in accordance with the presence of sulphate in the brine. However, the bacterial number was low, probably because the number of bacteria was reduced after removal from the geothermal plant. The specimen was exposed to oxygen for quite a long time, which could have significantly reduced the number of the bacteria present on the specimen. Also it was not optimal that the specimen was dried, because dehydratation also kills bacteria. Thus it is difficult to make any firm conclusions about the possibility for microbiologically induced corrosion.

CONCLUSIONS

The new Soultz EGS power plant is equipped with several km of steel pipes (casing, surface installations). Thus, corrosion and scaling issues have to be seriously taken into account either from laboratory experiments, on-site measurements and chemical modelling.

From laboratory experiments, the corrosion tests showed that carbon steel TU42BT corroded at 2 mm/y at 200°C. The corrosion products formed on the surface did not provide any protection against corrosion.

All the tested coatings performed very well. They effectively reduced the corrosion and they did not deteriorate during the test.

Mexel inhibitor did not reduce the corrosion rate significantly. The corrosion rate for TU42BT steel was nearly the same with and without the inhibitor.

It is probable that outside top part of the casing was subject to microbiological corrosion.

ACKNOWLEDGEMENT

Valuable discussion with Andre Gérard and Jean-Philippe Faucher is acknowledged. This work was financially supported by the EC project SES6-CT-2003-502706, EGS-Pilot Plant.

REFERENCES

Aquilina, L., Pauwels, H., Genter, A., Fouillac, C.: Water-rock interaction processes in the Triassic sandstone and the granitic basement of the Rhine Graben: geochemical investigation of a geothermal reservoir, 1997, Geochimica and Cosmochimica Acta, vol 61, 20, 4281-4295.

Baticci, F.: Material study on geothermal EGS (Enhanced Geothermal System) power plant: application to the Soultz-sous-Forêts site, 2009, Politecnico di Milano,

Facoltà di Ingegneria Industriale, Corso di Laurea in Ingegneria Meccanica, Diploma thesis, Italy, 202 pp.

Baticci, F., Faucher, J.-Ph.: Corrosion studies at Soultz: overview of the past results and on-going works, 2008, EHDRA scientific conference, Soultz-sous-Forêts, France, 24-25 September 2008, 16 pp.

Baticci, F., Genter, A., Huttenloch, P., Zorn, R.: Corrosion and scaling detection in the Soultz EGS power plant, Upper Rhine Graben, France, 2010, World Geothermal Congress, WGC2010, Bali, Indonesia, April 2010.

Fazio, P. (ed.), ASTM Standard Practice G 1 - 90, Standard Practice for Preparing, Cleaning, and Evaluating Corrosion Test Specimens, 1992, Annual Book of ASTM Standards, Vol. 03.02., American Society for Testing and Materials, s.35-41.

Fritsch, D., Baumgaertner, J., Cuenot, N., Graff, J.J., Genter, A.: The Soultz EGS pilot plant: energy heat and power from deep Enhanced Geothermal Systems, 2008, EVER08, March 27-30, 2008, Monte-Carlo (Monaco).

Genter, A., Evans, K.F., Cuenot, N., Fritsch, D., Sanjuan, B.: The geothermal Soultz adventure: 20 years of reconnaissance and research for exploring deep crystalline fractured rocks, 2010, Geoscience.

Genter, A., Fritsch, D., Cuenot, N., Baumgaertner, J., Graff, J.J.: Overview of the current activities of the European EGS Soultz project: from exploration to electricity production, 2009, 34th Stanford Reservoir Engineering Geothermal Workshop 2009, February 09-11 2009, San Francisco, California, USA, 163-169.

Gérard, A., Genter, A., Kohl, T., Lutz, Ph., Rose, P., Rummel, F.: The deep EGS (Enhanced Geothermal System) project at Soultz-sous-Forêts (Alsace, France), 2006, Geothermics, vol. 35, No 5-6, 473-483.

Hettkamp, T., Baumgaertner, J., Baria, R., Gérard, A., Gandy, T., Michelet, S., Teza, D.: Electricity production from Hot Rocks, 2004, In: 29th Workshop on Geothermal Reservoir Engineering, Stanford University, Stanford, California, USA, January 26-28, 2004, 184-193.

Lichti, K.A., Wilson, P.T., Inman, M.E.: Corrosivity of Kawerau geothermal steam, 1997, Geothermal Resources Council Transactions, 21, 25-32.

Lichti, K.A., Wilson, P.T.: Corrosion in New Zealand geothermal systems, 1999, Corrosion Reviews, 17, 181-203.

Nami, P., Schellschmidt, R., Schindler, M., Tischner, T.,: Chemical stimulation operations for reservoir development of the deep crystalline HDR/EGS system at Soultz-sous-Forêts (France), 2008, Proceedings, Thirty-Third Workshop on Geothermal Reservoir Engineering Stanford University, Stanford, California, USA, January 28-30, 2008, SGP-TR-185, 296-306.

Pauwels, H., Fouillac, C., Fouillac, A.-M.: Chemistry and isotopes of deep geothermal saline fluids in the Upper Rhine Graben: Origin of compounds and water-rock interactions, 1993, Geochimica and Cosmochimica Acta 57, 2737-2749.

Sampedro, J.A., Rosas, N., Diaz, R., Dominguez, B.: Developments in geothermal energy in Mexico – Part thirty. Conclusions of the corrosion in Mexican geothermal wells project, 1990, Heat Recovery Systems & CHP, 10, 481-490.

Sanada, N., Kurata, Y., Nanjo, H., Kim, H., Ikeuchi, J.: IEA deep geothermal resources subtask C: Materials, Progress with a database for materials performance in deep and acidic geothermal wells, 2000, Proceedings World Geothermal Congress, Kyushu – Tohoku, Japan, May 28 – June 10.

Sanjuan, B., Millot, R., Dezayes, Ch., Brach, M.: M main characteristics of the deep geothermal brine (5 km) at Soultz-sous-Forêts (France) determined using geochemical and tracer test data, 2010, Geoscience.

Sanjuan, B., Pinault, J.-L., Rose, P., Gérard, A., Brach, M., Braibant, G., Crouzet, C., Foucher, J.-C., Gautier, A., Touzelet, S.: Geochemical fluid characteristics and main achievements about tracer tests at Soultz-sous-Forêts (France), 2006, BRGM/RP-54776-FR report, 64 pp.

Vuataz, F.-D., Brach, M., Criaud, A., Fouillac, C.: Geochemical monitoring of drilling fluids: a powerful tool to forecast and detect formation waters, 1990, SPE, Formation Evaluation, 177-184.

Table 1. Test Matrix.

Test #	Solution	pH	t / ºC	MEXEL filming chemical / ppm	CO_2 /m	pCO_2 / bar	p_{total} / bar	Test duration
EGS_02	Soultz brine	4.8	200	-	0.03	0.5	15	1 week
EGS_03	Soultz brine	4.8	200	10	0.03	0.5	15	1 week

Table 2. Chemical Composition of the Tested Steels.

Steel#	C	Si	Mn	P	S	Cu
TU42BT	0.22	0.4	1.15	0.04	0.04	0.3
P110				0.03	0.03	
N80				0.03	0.03	

Table 3. Composition of the Produced Brine.

Ion	Concentration	
	mmol/l	mg/l
Na^+	1225.47	28173.56
K^+	73.66	2880.11
Mg^{2+}	3.09	75.12
Ca^{2+}	165.92	6650.07
Fe^{2+}	1.74	97.18
Cl^-	1630.47	57800.16
SO_4^{2-}	1.78	170.99
Total alkalinity	6.60	402.72

Table 4. Mass Loss Corrosion Rate for the Tested Materials.

Test #	Inhibitor	Specimen	Mass loss C.R. [mm/y]	Film mass [mg/cm^2]
EGS_02		TU42BT steel non-coated	1.8	4
		Sakaphen coating	0.03	N/a
		Red Teflon coating	Not detectable	N/a
		Green Teflon coating	Not detectable	N/a
EGS_03	MEXEL 10 ppm	TU42BT steel non-coated	1.4	9
		P110 non-coated	2.5	17
		N80 non-coated	2.5	14

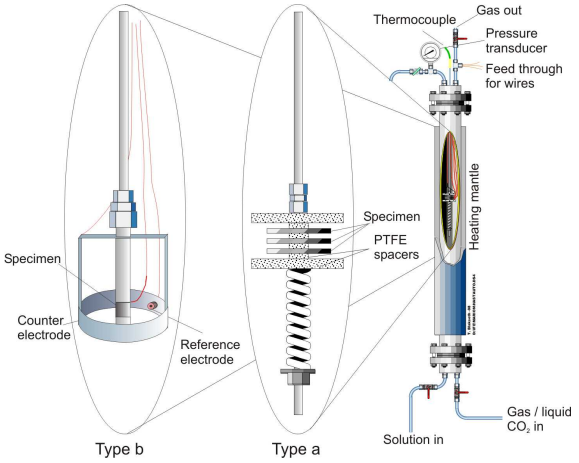

Figure 1: Schematic drawing of the autoclave

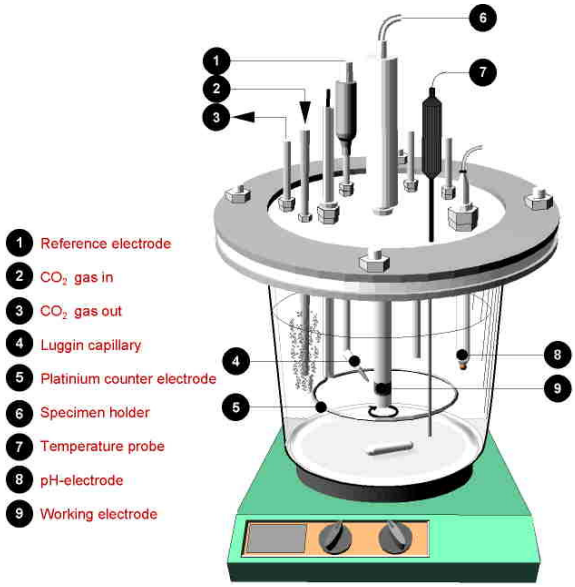

Figure 2: Schematic illustration of a glass cell with accessories

Figure 4: Photograph of the non-coated TU42BT steel specimen after test EGS_02. Test conditions:200 °C, 0.5 bar CO2, pH 4.6-5, brine (seeTable 3)

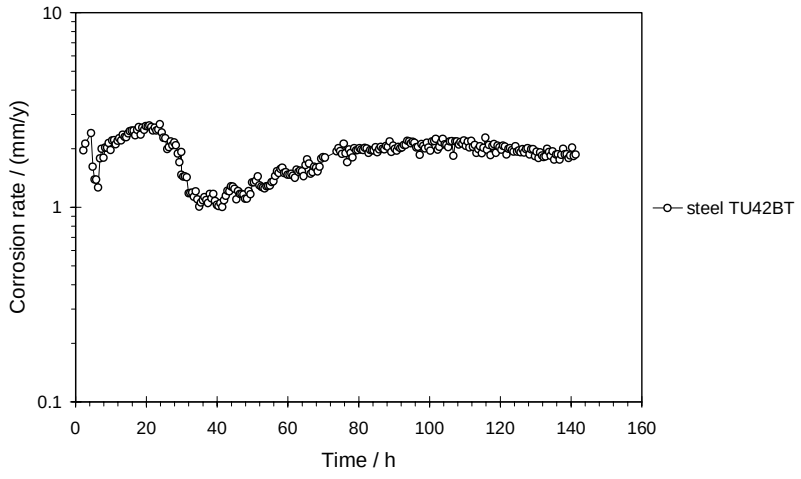

Figure 3: Corrosion rate versus time for the non-coated TU42BT steel specimen, test EGS_02. Test conditions: 200 °C, 0.5 bar CO2, pH 4.6-5,brine (see Table 3)

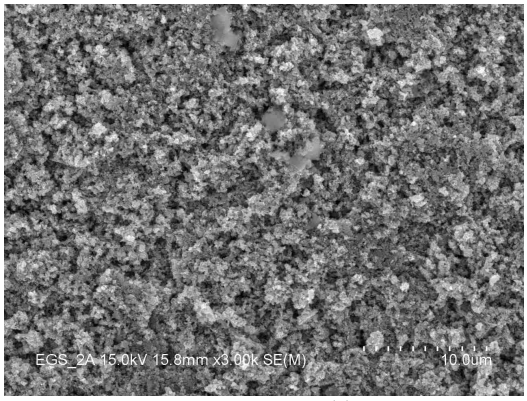

(a)

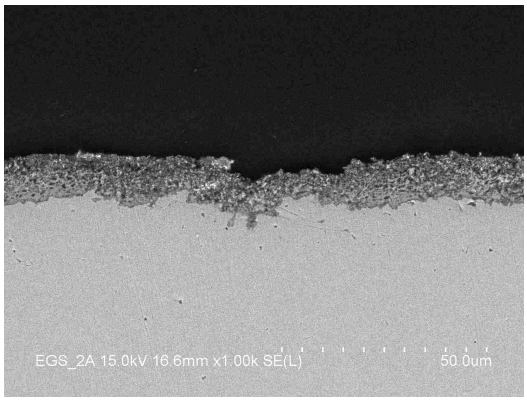

(b)

Figure 5: SEM images of the non-coated TU42BT steel specimen after test EGS_02 (a) specimen surface, (b) cross-section of the specimen. Test conditions: 200 °C, 0.5 bar CO2, pH 4.6-5, brine (see Table 3)

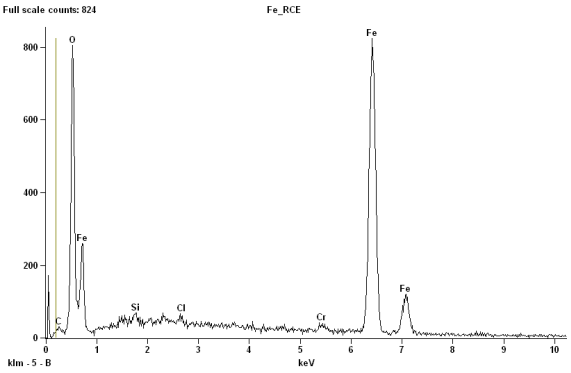

Quantitative Results EGS_02A

Element	*Weight %*	*Atom %*
C	4.11	9.19
O	37.25	62.47
Si	0.14	0.14
Cl	0.28	0.21
Cr	0.75	0.38
FeL	57.47	27.61
Total	100.00	100.00

Figure 6: EDS analysis of the corrosion product layer on the non-coated TU42BT steel specimen, test EGS_02. Test conditions: 200 °C, 0.5 bar CO2, pH 4.6-5, brine (see Table 3*)*

Figure 7: Photograph of the specimen coated with Sakaphen synthetic coating after test EGS_02. Test conditions: 200 °C, 0.5 bar CO2, pH 4.6-5, brine (see Table 3)

Figure 8: Photograph of the specimen coated with the red Teflon coating after test EGS_02. Test conditions: 200 °C, 0.5 bar CO2, pH 4.6-5, brine (see Table 3)

Figure 9: Photograph of the specimen coated with the green Teflon coating after test EGS_02. conditions: 200 °C, 0.5 bar CO2, pH 4.6-5, brine (see Table 3)

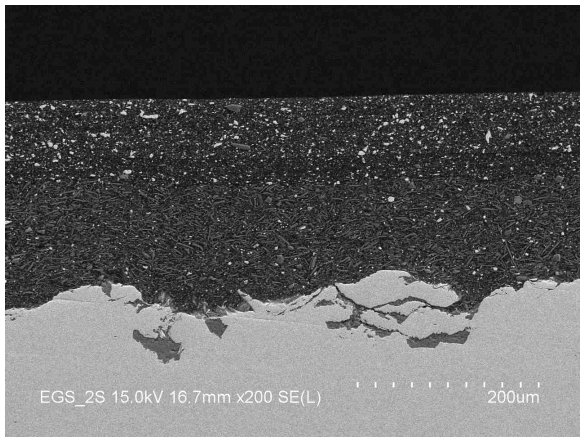

Figure 10: SEM image of a cross section of the specimen with Sakaphen synthetic coating, test EGS_02. Test conditions: 200 °C, 0.5 bar CO2, pH 4.6-5, brine (see Table 3)

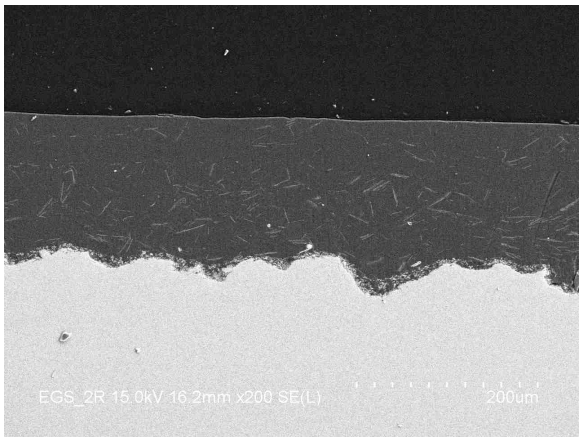

Figure 11: SEM image of a cross section of the specimen with the red Teflon coating, test EGS_02. Test conditions: 200 °C, 0.5 bar CO2, pH 4.6-5, brine (see Table 3)

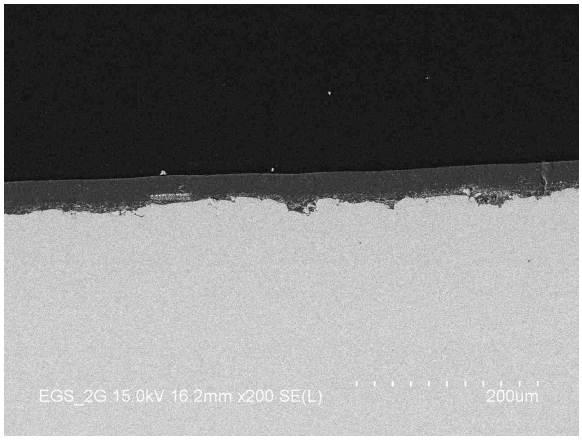

Figure 12: SEM image of a cross section of the specimen with the green Teflon coating, test EGS_02. Test conditions: 200 °C, 0.5 bar CO2, pH 4.6-5, brine (see Table 3)

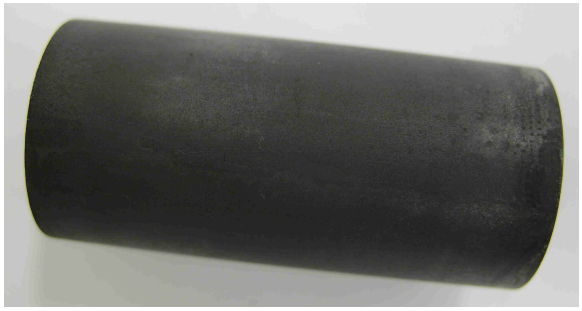

Figure 14: Photograph of the non-coated TU42BT steel specimen after test EGS_03. Test conditions: 200 °C, 0.5 bar CO2, pH 4.6-5, brine (see Table 3), 10 ppm Mexel inhibitor

Figure 15: Photograph of the non-coated P110 steel specimen after test EGS_03. Test conditions: 200 °C, 0.5 bar CO2, pH 4.6-5, brine (see Table 3), 10 ppm Mexel inhibitor

Figure 16: Photograph of the non-coated N80 steel specimen after test EGS_03. Test conditions: 200 °C, 0.5 bar CO2, pH 4.6-5, brine (see Table 3), 10 ppm Mexel inhibitor

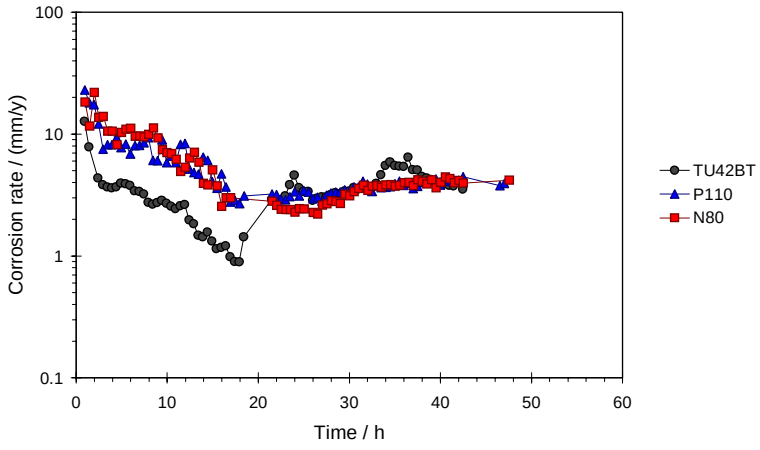

Figure 13: Corrosion rate versus time for the non-coated steel specimens, test EGS_03. Test conditions: 200 °C, 0.5 bar CO2, pH 4.6-5, brine (see Table 3), 10 ppm Mexel inhibitor

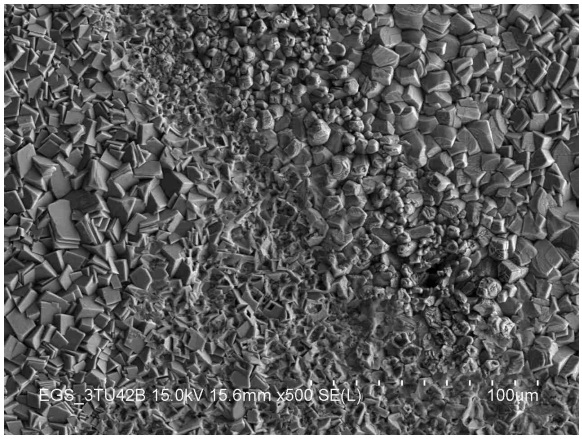

(a)

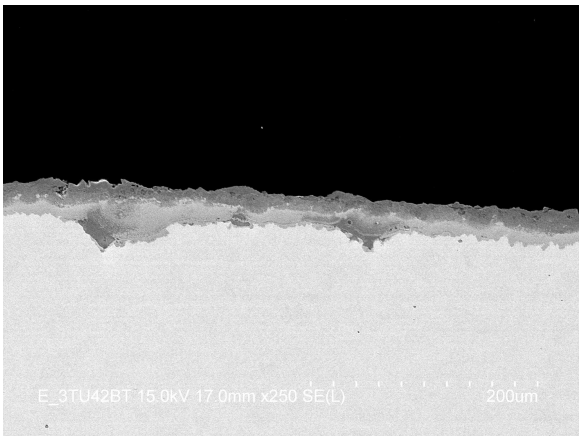

(b)

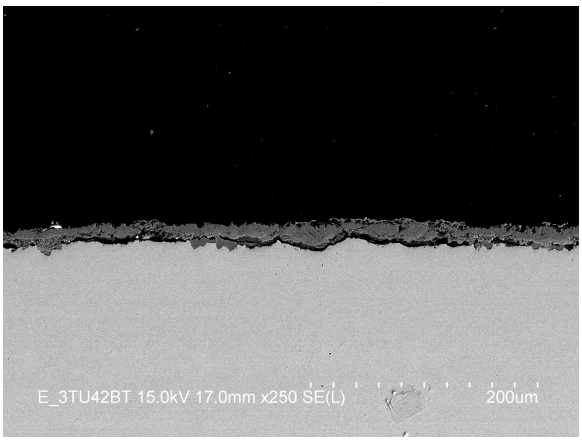

(c)

Figure 17: SEM images of the non-coated TU42BT steel specimen after test EGS_03 (a) specimen surface (b-c) cross sections of the specimen. Test conditions: 200 °C, 0.5 bar CO2, pH 4.6-5, brine (see Table 3), 10 ppm Mexel inhibitor

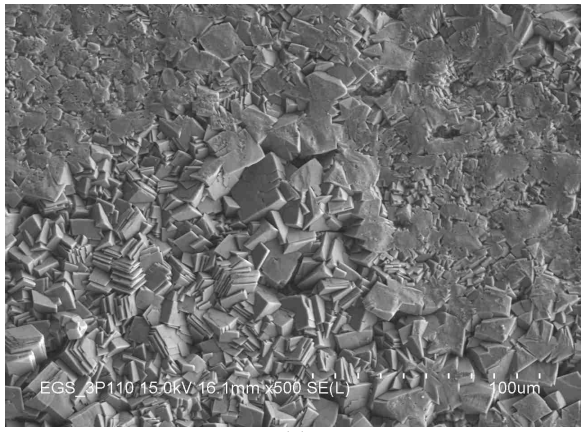

(a)

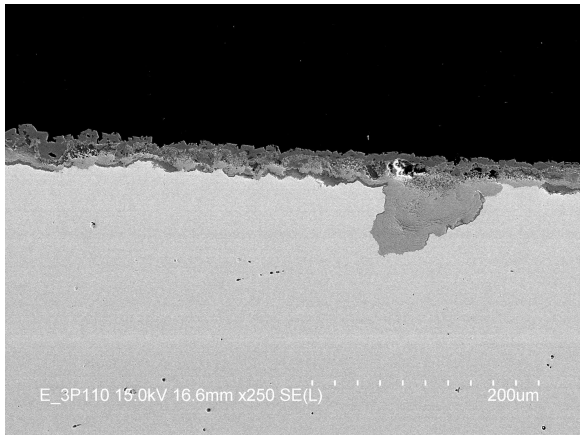

(b)

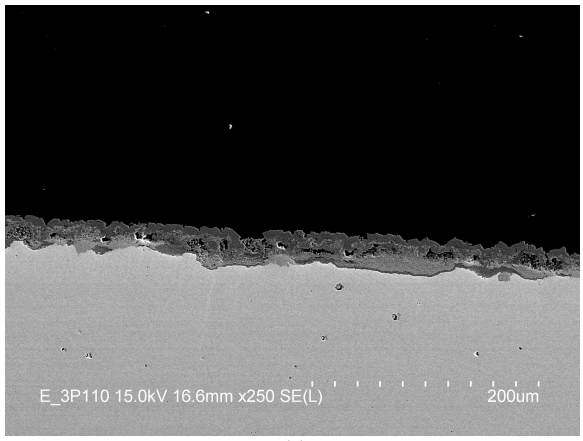

(c)

Figure 18: SEM images of the non-coated P110 steel specimen after test EGS_03 (a) specimen surface (b-c) cross sections of the specimen. Test conditions: 200 °C, 0.5 bar CO2, pH 4.6-5, brine (see Table 3), 10 ppm Mexel inhibitor

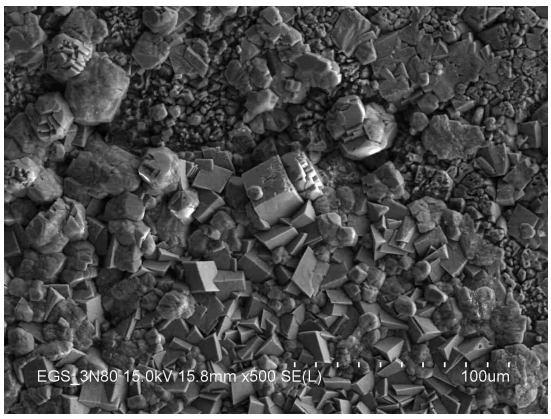

(a)

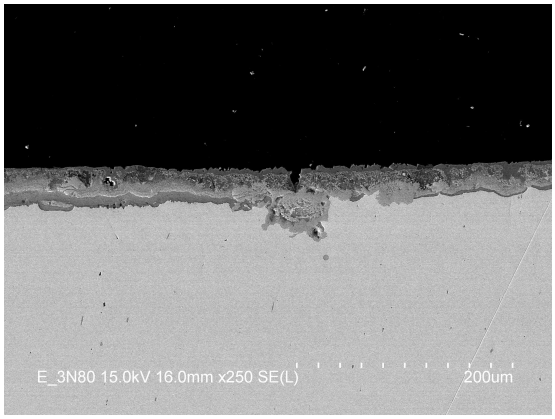

(b)

Figure 19: SEM images of the non-coated N80 steel specimen after test EGS_03 (a) specimen surface (b) cross section of the specimen. Test conditions: 200 °C, 0.5 bar CO2, pH 4.6-5, brine (see Table 3), 10 ppm Mexel inhibitor

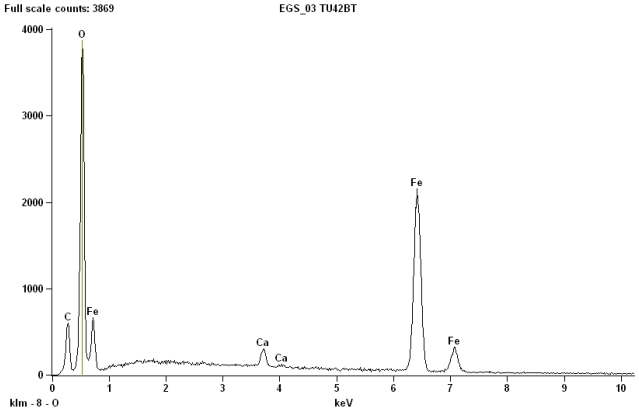

Quantitative Results EGS_03 TU42BT

Element	*Weight %*	*Atom %*
C	***13.11***	***23.49***
O	***44.62***	***60.05***
Ca	***1.08***	***0.58***
Fe	***41.19***	***15.88***
Total	***100.00***	***100.00***

Figure 20: EDS analysis of the corrosion product layer on the non-coated TU42BT steel specimen, test EGS_03. Test conditions: 200 °C, 0.5 bar CO2, pH 4.6-5, brine (see Table 3), 10 ppm Mexel inhibitor

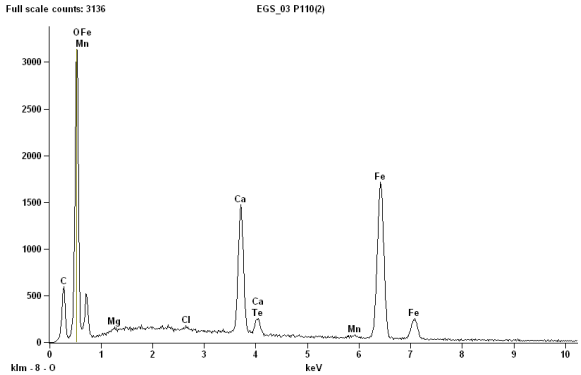

Quantitative Results EGS_03 P110(2)

Element	**Weight%**	**Atom%**
C	**12.14**	**21.49**
O	**46.24**	**61.44**
Mg	**0.12**	**0.11**
Ca	**7.89**	**4.19**
Fe	**33.55**	**12.77**
Total	**99.94**	**99.99**

Figure 21: EDS analysis of the corrosion product layer on the non-coated P110 steel specimen, test EGS_03. Test conditions: 200 °C, 0.5 bar CO2, pH 4.6-5, brine (see Table 3), 10 ppm Mexel inhibitor

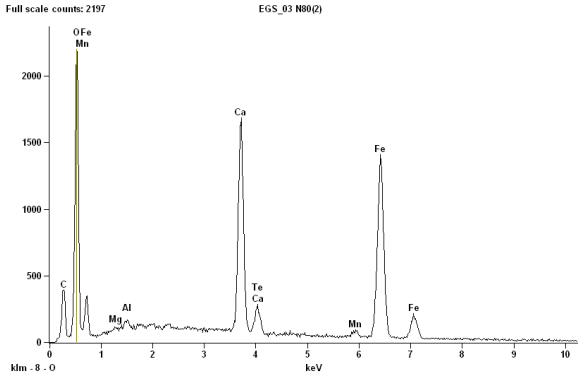

Quantitative Results EGS_03 N80(2)

Element	***Weight%***	***Atom%***
CK	10.96	19.55
OK	46.54	62.29
MgK	0.09	0.08
AlK	0.24	0.19
CaK	11.71	6.26
FeL	30.24	11.60
Total	99.78	99.96

Figure 22: EDS analysis of the corrosion product layer on the non-coated N80 steel specimen, test EGS_03. Test conditions: 200 °C, 0.5 bar CO2, pH 4.6-5, brine (see Table 3), 10 ppm MexelL inhibitor

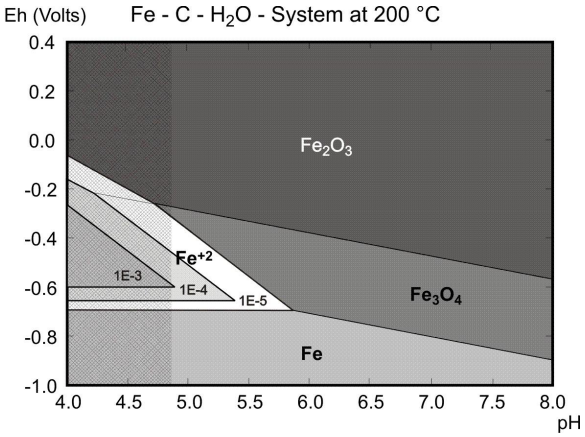

Figure 24: Eh-pH diagram (Pourbaix diagram) for Fe-C-O at 200°C in the pH range 4-8. The diagram is for 20bar, 0.03 m carboneous species and a Fe2+ concentration of 10-3, 10-4 and 10-5m. The hatched area indicates thee pH range for the experiments. (Constructed with HSC Chemistry 6.1. Outotec Research Oy Information Center, P.O. Box 69. FIN - 28101 PORI, FINLAND)

Figure 26: Photograph of the corroded part of the pack-off assembly of casing in the injection well GPK3 suspected for microbiological corrosion

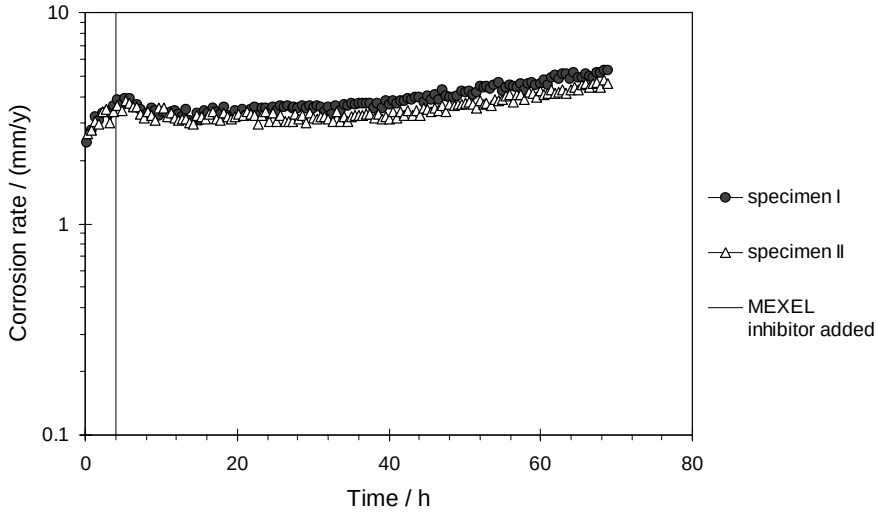

Figure 23: Corrosion rate versus time for the non-coated steel specimen, test EGS_04. Test conditions: 60 °C, 0.75 bar CO2, pH 4.8-5, brine (see Table 3), 10 ppm Mexel inhibitor

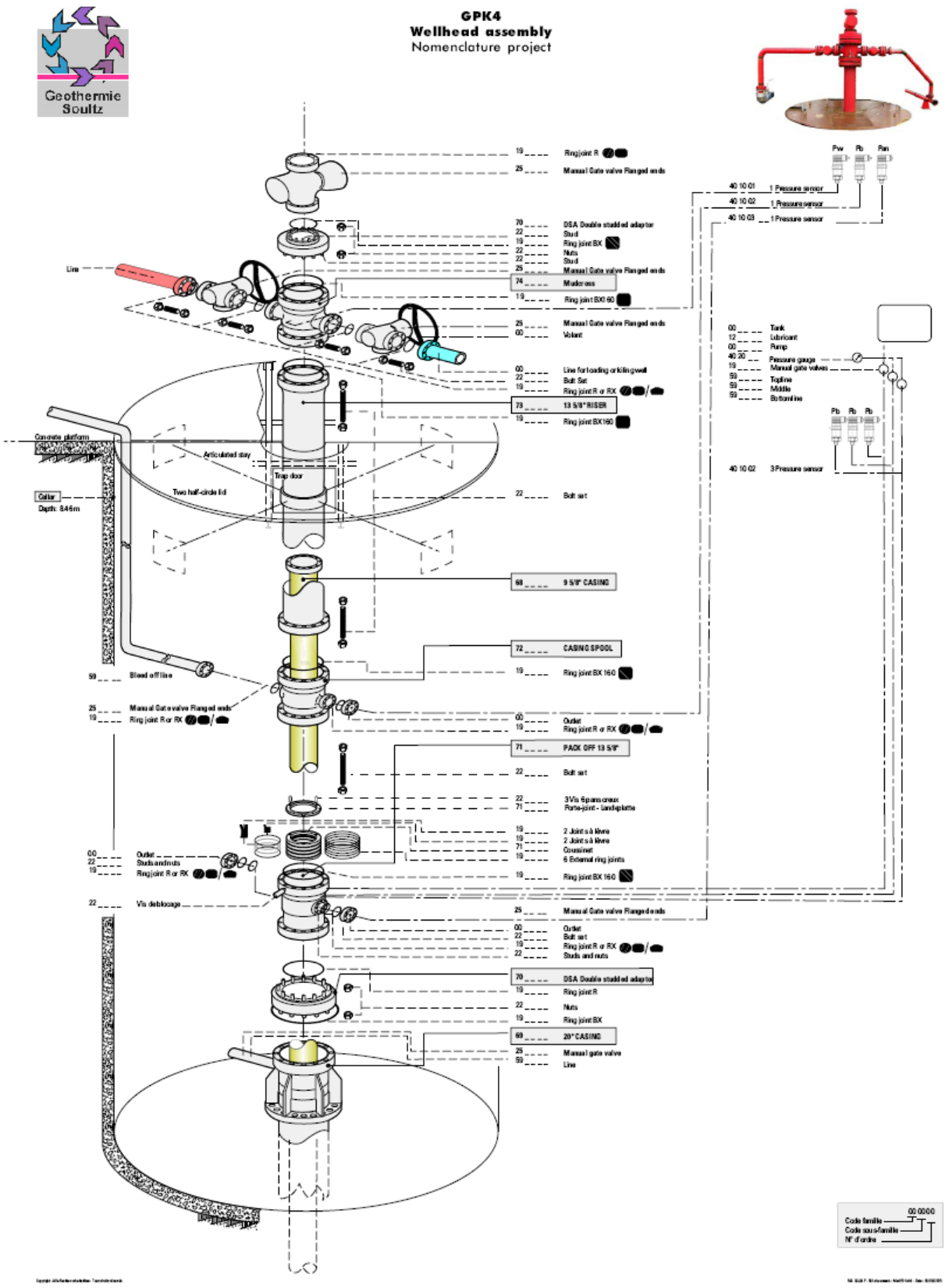

Figure 25: Well head assembly where the suspected microbiologically induced pitting corrosion was found